THE JOURNAL OF PHYSICAL CHEMISTRY B

Article

pubs.acs.org/JPCB

Ab Initio Liquid Water Dynamics in Aqueous TMAO Solution

Kota Usui,[†] Johannes Hunger,[†] Marialore Sulpizi,[‡] Tatsuhiko Ohto,[§] Mischa Bonn,[†] and Yuki Nagata*[,†]

[†]Max Planck Institute for Polymer Research, Ackermannweg 10, D-55128 Mainz, Germany

[‡]Johannes Gutenberg University Mainz, Staudingerweg 7, 55099 Mainz, Germany

[§]Graduate School of Engineering Science, Osaka University, 1-3 Machikaneyama, Toyonaka, Osaka 560-8531, Japan

ABSTRACT: *Ab initio* molecular dynamics (AIMD) simulations in trimethylamine *N*-oxide (TMAO)−D_2O solution are employed to elucidate the effects of TMAO on the reorientational dynamics of D_2O molecules. By decomposing the O−D groups of the D_2O molecules into specific subensembles, we reveal that water reorientational dynamics are retarded considerably in the vicinity of the hydrophilic TMAO oxygen (O_{TMAO}) atom, due to the O−D···O_{TMAO} hydrogen-bond. We find that this reorientational motion is governed by two distinct mechanisms: The O−D group rotates (1) after breaking the O−D···O_{TMAO} hydrogen-bond, or (2) together with the TMAO molecule while keeping this hydrogen-bond intact. While the orientational slow-down is prominent in the AIMD simulation, simulations based on force field models exhibit much faster dynamics. The simulated angle-resolved radial distribution functions illustrate that the O−D···O_{TMAO} hydrogen-bond has a strong directionality through the sp^3 orbital configuration in the AIMD simulation, and this directionality is not properly accounted for in the force field simulation. These results imply that care must be taken when modeling negatively charged oxygen atoms as single point charges; force field models may not adequately describe the hydration configuration and dynamics.

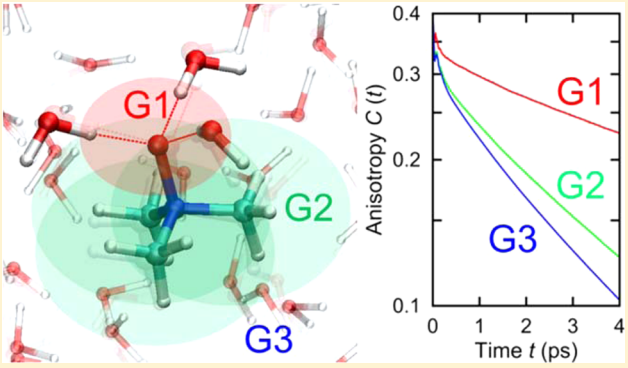

I. INTRODUCTION

Trimethylamine *N*-oxide (TMAO) is an amphiphilic organic molecule which contains both hydrophilic and hydrophobic parts. In aqueous TMAO solutions, the hydrophilic oxygen atom (O_{TMAO}) forms hydrogen-bonds with water molecules, and three methyl groups act as hydrophobic moieties. Aqueous TMAO solutions are biologically important, because they offer unique environments for living cells and affect biologically relevant processes: The TMAO molecule stabilizes the structures of proteins[1−3] and RNA,[4] and counteracts the destabilization of proteins due to urea.[5,6] In muscle tissue of deep-sea animals, the concentration of TMAO is significantly enhanced, ameliorating the detrimental effects of hydrostatic and osmotic pressures on enzyme function.[7−9] It has been proposed that TMAO is generally excluded from protein surfaces, which implies that the stabilization effect of TMAO on proteins is mediated by in-between water molecules, rather than by direct TMAO−protein interactions.[10−15] This manifests the complexity of the mechanism by which TMAO stabilizes biomacromolecules.[1,6,10,16−23] Thus, a molecular level understanding of the TMAO−water interactions is important to clarify the role of TMAO in biologically relevant processes. Furthermore, the understanding will be useful for investigating the interfacial water structure and dynamics near the surfactant monolayer composed of zwitterionic lipid.[24]

Intermolecular interactions between TMAO and water have been investigated by theoretical[1,6,10,19,21,25−37] as well as several experimental approaches, including linear infrared (IR),[19,35,38,39] mid-IR pump−probe,[40−42] two-dimensional IR,[43] Raman,[44,45] NMR,[36,46] and dielectric relaxation[38,47] spectroscopy. By probing the O−D groups in isotopically diluted water in a polarization- and time-resolved IR scheme, Rezus and Bakker have shown that the water reorientational dynamics in aqueous TMAO solutions slows down with increasing the TMAO concentration.[40] Since this slow-down motion was also observed in various hydrophobic solutes, it was concluded that the retardation of water rotation stems from water molecules that hydrate the hydrophobic methyl groups. The slow-down near the hydrophobic parts of these molecules has been challenged by NMR experiments,[46] force field MD simulations of aqueous TMAO solution,[29] and AIMD simulations of aqueous methanol solution, which reported that the slow-down of the water motion near the hydrophobic parts was rather limited.[48] A further time-resolved IR study[42] has indicated that the slow-down of water dynamics is less pronounced near the hydrophobic parts than near the hydrophilic parts. In particular, for aqueous solutions of TMAO, the interaction of water molecules with the hydrophilic O_{TMAO} atom has been suggested to dominate the slow-down of water dynamics.[42,49] This strong hydrogen-bonding interaction of water molecules with the negatively charged O_{TMAO} atom is evidenced by a pronounced red-shifted of the O−D stretch vibration in the IR absorption

Received: March 17, 2015
Revised: July 2, 2015
Published: July 14, 2015

DOI: 10.1021/acs.jpcb.5b02579
J. Phys. Chem. B 2015, 119, 10597−10606

spectra by well over 100 cm^{-1} with respect to the peak frequency of neat water without TMAO.[19,50] By exciting the O−D stretching mode at a frequency of 2440 cm^{-1} in an IR pump−probe experiment, some of us probed the rotational dynamics of the O−D groups hydrogen-bonded to the hydrophilic group of the TMAO molecule.[42] The data for concentrated TMAO solutions reveal that the O−D chromophores characterized by this low stretching frequency reorient very slowly, which indicates that the O−D groups interact very strongly with the hydrophilic groups and are nearly immobile. This was supported by dielectric relaxation experiments which suggested that TMAO strongly binds, at all concentrations, 2−3 water molecules.

MD simulations have revealed that the water reorientational motion in liquid water can be explained with the angular jump model.[51] For a water molecule to rotate, it needs to break its existing hydrogen-bond, and make a new one. A new hydrogen-bonding partner therefore has to approach the water molecule, so that a short-lived bifurcated hydrogen-bond is formed. To relate the retarded reorientational dynamics of water molecules near TMAO to the angular jump model, Laage and co-workers have performed force field MD simulations of aqueous TMAO solutions[28,29,51−57] with the SPC/E water model[58] and the TMAO force field model.[59] They found that the reorientation of water molecules is only very moderately slowed down by the presence of TMAO molecules in aqueous TMAO solutions.[29] This moderate slowing down was attributed to the excluded volume effect of the TMAO molecule.[29] Due to the presence of the TMAO, water molecules near the solute lose possible hydrogen-bond partners, preventing the water molecules from rotating. The force field MD simulations by Laage et al. further indicate that the slow-down of water dynamics does not result from an iceberg structure of water near the hydrophobic part of the TMAO molecule and that the hydrophilic part of the TMAO molecule should contribute to the slowing down of the water reorientational motions.[28] No iceberg structure around the hydrophobic part of TMAO had previously been concluded from NMR studies.[46]

Force field MD simulations rely on the point charges and van der Waals interaction parameters used in the force field model, which represents the intermolecular interactions, here specifically between water and TMAO. It is challenging to gauge the quality of the force field model for the water and TMAO molecules, but it is apparent that in order to capture all details of TMAO−water interaction the red-shift of the stretch mode of the O−D groups in the presence of TMAO, i.e., of the O−D···O_{TMAO} group, should be reproduced by the model. The force field MD simulation predicts a ∼30 cm^{-1} red-shift, which is appreciably smaller than the experimentally observed red-shifts (exceeding 100,[19,50] ∼55,[42] and 290 cm^{-1}[39]), indicating that the O−D···O_{TMAO} hydrogen-bond strength is underestimated in the force field MD simulation. In fact, density functional theory (DFT) calculations of a system consisting of one TMAO molecule and three water molecules predicted that the atomic charges on the O_{TMAO} atom reduces considerably, by ∼10%, upon formation of the O−D···O_{TMAO} hydrogen-bond,[60] which is difficult to include in classical force fields. This suggests that *ab initio* modeling is required to examine the effect of the hydrophilic group of the TMAO molecule on the water dynamics.

In this paper, we perform *ab initio* MD (AIMD) and force field MD simulations for a mixture of TMAO and D_2O and for neat D_2O and explore the orientational dynamics of water molecules near the TMAO molecule. AIMD has been a unique tool to capture the liquid dynamics; it has been shown that AIMD in the bulk water can capture cooperative hydrogen-bond dynamics which is missing in force field MD simulaton.[61,62] By specifically studying the O−D groups interacting with the O_{TMAO} atom and with the hydrophobic methyl groups, we identify the different contributions of these O−D groups to the vibrational density of states and the rotational dynamics. Our AIMD simulation shows that the O−D groups interacting with the O_{TMAO} atom contribute to a vibrational density of states centered at 2300 cm^{-1}, i.e., strongly red-shifted, consistent with experiments.[19,39,42,50] The hydrogen-bond lifetimes of these TMAO−water bonds are exceptionally long, and thus, these O−D groups show much slower rotational dynamics compared to those in the pure D_2O. The slow rotational dynamics of O−D groups in the O−D···O_{TMAO} complex arises from the following two mechanisms. While the O−D···O_{TMAO} hydrogen-bond remains intact, the O−D group rotates together with the TMAO molecule. Alternatively, the O−D···O_{TMAO} hydrogen-bond is broken, and the O−D group moves away from the TMAO molecule, and sequentially rotates in the same fashion as in the bulk.

We compare these AIMD results with the results obtained from force field MD simulation and find that the slow dynamics of O−D groups interacting with the O_{TMAO} atom is not prominent in the force field MD simulations. We attribute this difference between the force field MD and AIMD to the oversimplified point charge model used in the former approach, which cannot describe the orbital directionality resulting from the sp^3 configuration near the O_{TMAO} atom. Finally, we briefly discuss the effects of the DFT functional/basis set on the water dynamics in the TMAO−D_2O solution.

This paper is organized as follows. In section II, the protocols used for the AIMD and force field MD simulations are described. In section III, we discuss the simulated vibrational density of states, rotational dynamics, hydrogen-bond lifetime, and angle-resolved radial distribution functions (RDFs) calculated from the AIMD and force field MD trajectories. The effects of the DFT functionals and basis sets on the water dynamics near the TMAO molecule are also discussed in this section. Section IV is devoted to the conclusions.

II. METHODS

II.A. Simulation Protocols. We performed AIMD and force field MD simulations of the deuterated TMAO (dTMAO)−D_2O mixture and pure D_2O. The simulation cell size for the TMAO−D_2O mixture was set to 14.62 Å × 14.62 Å × 14.62 Å. The cell contained 1 dTMAO molecule and 100 D_2O molecules (corresponding to a TMAO molar concentration of 0.532 mol/L), resulting in a density of 1.109 g/cm^3. This density is based on literature values for solutions of TMAO in H_2O.[42,63] To take the isotope exchange into account we assume the molar volumes of water and TMAO to be independent of isotope exchange. The cell size used for the pure D_2O simulations was 12.429 Å × 12.429 Å × 12.429 Å. The cell contained 64 D_2O molecules, yielding a density of 1.108 g/cm^3. In both cases, periodic boundary conditions were employed, and the system temperature was set to 320 K in the canonical ensembles by using the thermostats of canonical sampling through velocity rescaling.[64] This temperature was used in both the AIMD and force field MD simulations. The simulations were performed with the CP2K software package.[65] The time step of 0.5 fs was used for both AIMD and force field MD simulations.

DOI: 10.1021/acs.jpcb.5b02579
J. Phys. Chem. B 2015, 119, 10597−10606

II.B. AIMD. We performed Born−Oppenheimer AIMD simulations with different functionals and basis sets. For the exchange and correlation functionals, we used the Becke−Lee−Yang−Parr (BLYP)[66,67] and revised Perdew−Burke−Ernzerhof (revPBE) functionals,[68] together with the van der Waals correction of the Grimme's D3 method.[69] The van der Waals corrections are crucial to reproduce the correct water density and dynamics.[70−72] We employed the Goedecker−Teter−Hutter pseudopotentials[73] and the hybrid Gaussian and plane waves method implemented in QUICKSTEP.[74] The DZVP and TZV2P basis sets were used for the Gaussian wave functions, while a density cutoff of 400 Ry was used for the plane waves.[75] We performed the simulations at the BLYP/DZVP, BLYP/TZV2P, and revPBE/TZV2P levels of theory to investigate the effects of the DFT functionals and the basis sets on water dynamics.

For the dTMAO−D_2O simulations, two different sets of initial coordinates were obtained from the force field MD trajectories, and we performed 15 ps (BLYP/DZVP, BLYP/TZV2P) and 20 ps NVT runs (revPBE/TZV2P) for equilibrating the systems. From the subsequent AIMD runs, we obtained total 477 ps (BLYP/DZVP), 643 ps (BLYP/TZV2P), and 320 ps (revPBE/TZV2P) AIMD trajectories, which were used for analyses. For the pure D_2O simulations, one set of initial coordinates was generated by the force field MD simulation. With this initial configuration, we performed 35 ps (BLYP/DZVP), 50 ps (BLYP/TZV2P), and 40 ps (revPBE/TZV2P) runs for equilibration. Sequentially, we obtained 266 ps (BLYP/DZVP), 457 ps (BLYP/TZV2P), and 374 ps (revPBE/TZV2P) AIMD trajectories. These were used for the analyses.

II.C. Force Field MD. For the force field MD simulations of the dTMAO−D_2O mixture and pure D_2O, the flexible SPC water model (SPC/Fw[76]) and flexible force field model of the TMAO molecule[59] were used. After 100 ps equilibrations, we obtained 1.4 and 0.4 ns MD trajectories for the dTMAO−D_2O mixture and pure D_2O, respectively. These MD trajectories were used for the analyses.

II.D. Categorization of O−D Groups. Since we aim at elucidating the effects of hydrophilic and hydrophobic parts of the TMAO molecule on the orientational dynamics of the O−D groups, we geometrically categorized the total of 200 O−D groups of D_2O in the aqueous dTMAO solutions into three subensembles (G1, G2, and G3). Ensemble G1 consists of the O−D groups that are hydrogen-bonded to the O_{TMAO} atom: an O−D group belongs to G1 when the intermolecular distance of $O_{TMAO}\cdots D_{D2O}$ is less than 2.27 Å.[77,78] Note that for discussion of the results below we further narrow down group G1 to subgroup G1′, which contains all O−D groups of G1, which keep their hydrogen-bond to the O_{TMAO} atom within the simulated time. Ensemble G2 comprises the O−D groups that are close to the hydrophobic methyl groups of the TMAO molecule: an O−D group is categorized into G2 when the O−D group is not categorized into G1 and the D_{D2O} atom is within a 5.0 Å radius from the buried carbon atoms of the dTMAO molecule. The cutoff of 5.0 Å was also used in a previous Car−Parrinello MD study on aqueous tetramethylurea solutions.[79] Note that the cutoff radius of 5.0 Å used for the G2 categorization is larger than that of 2.27 Å for the G1 categorization, because the G2 cutoff radius has been defined not from the outmost hydrogen atom but from the buried carbon atom, while the cutoff radius for G1 was defined from the O_{TMAO} atom. Ensemble G3 contains the rest of the O−D groups. Note that G1, G2, and G3 are mutually exclusive. Our AIMD simulation predicted that, on average, 2.9 O−D groups belonged to G1, which is comparable with the numbers of 2 (dielectric relaxation measurement,[47] nuclear Overhauser effect measurement,[80] and thermodynamics analysis[23]) and 2−3 (dielectric measurement[42]). The average numbers of O−D groups categorized into G1, G2, and G3 are summarized in Table 1.

Table 1. Average Number of the O−D Groups Contained in Subensembles G1, G2, and G3 in AIMD and Force Field MD Simulations

	BLYP/DZVP	BLYP/TZV2P	revPBE/TZV2P	force field
G1	2.9	2.9	2.9	2.5
G2	46.5	47.1	46.8	47.0
G3	150.6	150.0	150.3	150.5

III. RESULTS

III.A. Vibrational Density of States. To examine the red-shift of the vibrational spectral signature for the O−D chromophores interacting with the TMAO molecule, we calculated the vibrational density of states (VDOS) of the O−D stretch mode. The VDOS, $R(\omega)$, can be calculated from Fourier transform of the velocity autocorrelation function as

$$R(\omega) = \int_0^{\tau_{cut}} \langle \mathbf{v}_{OD}(t)\cdot\mathbf{v}_{OD}(0)\rangle e^{-i\omega t}\, dt \quad (1)$$

where $\boldsymbol{v}_{OD}(t)$ denotes the relative velocity of the D atom of the D_2O molecule with respect to the O atom on the same D_2O at time t. The time correlation was cut at time τ_{cut}, which was set to 1 ps in this study. $\langle\cdots\rangle$ denotes the thermal average. The calculated VDOS for subensembles G1 (near hydrophilic group of the TMAO molecule) and G2 (near hydrophobic groups) are shown in Figure 1 as well as the VDOS for the pure D_2O.

The VDOS of the G1 O−D groups exhibit an O−D stretch peak centered at 2300 cm^{-1}, indicating that the strongly red-shifted (~160 cm^{-1}) frequency arises from the O−D groups that are hydrogen-bonded to the O_{TMAO} atom, which is in line with experimental results.[19,50] The VDOS for the G2 O−D groups is similar to that of the pure D_2O, indicating that the hydrogen-bond strength of the G2 O−D groups is similar to that in the bulk D_2O. Note that this ~160 cm^{-1} red-shift of the O−D stretch mode is not observed in the force field MD simulation,[28] demonstrating that AIMD simulations yield substantially stronger interaction of water with O_{TMAO}, compared to force field MD simulations.

Note that the width of the G1 VDOS is broad, although the G1 O−D groups are strongly hydrogen-bonded and thus exhibit little structural inhomogeneity (see discussion of the radial distribution functions (RDFs) below and corresponding Figure 6). The broad VDOS with simultaneous narrow distribution of binding configurations arises from the high sensitivity of the frequency to the hydrogen-bond strength at red-shifted O−D (O−H) stretch frequencies.[81]

III.B. Rotational Dynamics. The anisotropy decay of the O−D groups, which are accessible from time-resolved IR experiments, can be directly related to the time correlation function[82]

$$C_2(t) = \frac{2}{5}\left\langle P_2\left(\frac{\mathbf{r}_{OD}(t)\cdot\mathbf{r}_{OD}(0)}{|\mathbf{r}_{OD}(t)||\mathbf{r}_{OD}(0)|}\right)\right\rangle \quad (2)$$

DOI: 10.1021/acs.jpcb.5b02579
J. Phys. Chem. B 2015, 119, 10597−10606

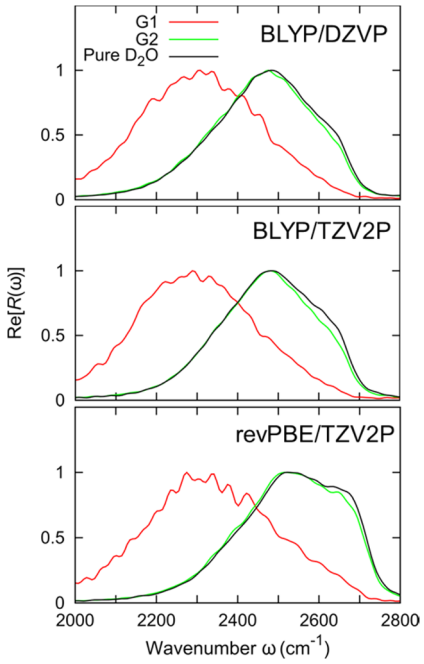

Figure 1. Real parts of the calculated VDOS, $R(\omega)$, for the G1 and G2 O−D groups in the TMAO−D_2O solution. The VDOS of the pure D_2O is also plotted.

where $\boldsymbol{r}_{OD}(t)$ denotes the vector of the O−D group of the D_2O molecule at time t, and $P_2(x) = (1/2)(3x^2 - 1)$ is the second Legendre polynomial. This expression was used for calculating the anisotropy decay of pure D_2O. To examine the anisotropy decays for the subensembles G1, G2, and G3 in the aqueous TMAO solution, we used the time correlation function

$$C_{Gi}(t) = \frac{2}{5}\left\langle P_2\left(\frac{\mathbf{r}_{OD}(t)\cdot\mathbf{r}_{OD}(0)}{|\mathbf{r}_{OD}(t)||\mathbf{r}_{OD}(0)|}\right)\theta_{Gi}(0)\right\rangle \quad (3)$$

where $\theta_{Gi}(t)$ is a step function with value 1 when the D atom of the O−D bond is found in Gi at time t, and otherwise 0.

$C_{G1}(t)$, $C_{G2}(t)$, and $C_{G3}(t)$ calculated from the simulations are shown in Figure 2. This figure directly shows that the

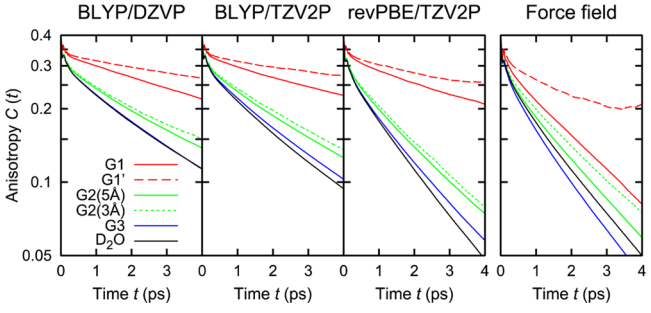

Figure 2. Semilog plots of simulated anisotropy decays of the G1, G2, and G3 O−D groups in the aqueous TMAO solutions, together with the decays of the O−D groups in pure D_2O.

rotational dynamics of the G3 O−D groups are similar to that in the pure D_2O, meaning that the G3 O−D groups behave like bulk O−D groups and the effect of the TMAO molecule on the orientational motion is negligible in the second hydration shell and beyond. This is consistent with an earlier Car−Parrinello MD study on the effect of the amphiphile tetramethylurea on water dynamics.[79,83] The G2 O−D groups show slower reorientational dynamics compared with those in the bulk D_2O, which is also in line with the previous force field based MD simulations.[29,79] These results thus indicate a moderate slow-down of the rotational dynamics within the hydrophobic hydration shell of TMAO. We note that the magnitude of the slow-down depends on the number of water molecules defined to be in the G2 ensemble: using a cutoff of 3.0 Å for the G2 categorization instead of 5.0 Å, with which the subensemble G2 contains ∼5 O−D chromophores, the G2 dynamics becomes slightly retarded (see Figure 2). From single exponential fits to the anisotropy decays, we find a retardation of ∼1.1−1.3 (5 Å cutoff) and ∼1.2−1.4 (3 Å cutoff). Though the exact definition of G2 makes comparison to different experimental values not straightforward, our results do not provide evidence for a very marked immobilization of water molecules at dilute concentrations, i.e., on time scales exceeding 10 ps.[40] The moderate slow-down is in broad accordance with recent studies using force field MD simulations (retardation 1.3−1.5),[29] NMR relaxometry[46] (retardation 1.6), and a combined dielectric relaxation and fs-IR study (retardation 2.8) at similarly low concentrations of TMAO. The AIMD simulations show remarkably slower dynamics of the G1 O−D groups than that in the pure D_2O. Note that this slowing down is not so pronounced in the force field MD simulation. We will address the qualitative difference between the AIMD and force field MD simulations in section III.D. For all types of O−D groups, there is a fast initial decay due to the librational motion of the water molecules followed by a slower decay, resulting from reorientation.

The question presents itself: What governs the slow rotational motion of the G1 O−D groups? Here, two distinct molecular mechanisms can be operative, which are illustrated in Figure 3:

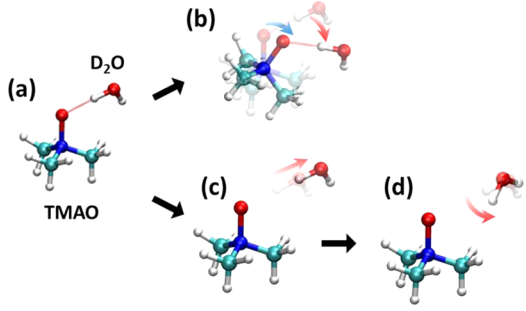

Figure 3. Two mechanisms for the G1 O−D groups to lose the orientational information. The upper route (a to b) shows that the O−D group keeps the O−D···O_{TMAO} hydrogen-bond intact and rotates as the TMAO + D_2O complex (denoted as subensemble G1′), while the lower pathway (a, c, to d) shows the mechanism by which reorientation occurs by breaking of the hydrogen-bond and subsequent rotation of the O−D group.

(i) The O−D group rotates by keeping the O−D···O_{TMAO} hydrogen-bond intact, or (ii) the hydrogen-bond is broken within t < 4 ps, and the O−D group dissociates from the TMAO molecule, resulting in its rotation independent of the TMAO molecule. To unravel the contributions from these two different scenarios, we calculated the rotational dynamics of those G1 O−D groups which keep the O−D···O_{TMAO} hydrogen-bond intact (G1′), by using the equation

$$C_{G1'}(t) = \frac{2}{5}\left\langle P_2\left(\frac{\mathbf{r}_{OD}(t)\cdot\mathbf{r}_{OD}(0)}{|\mathbf{r}_{OD}(t)||\mathbf{r}_{OD}(0)|}\right)\prod_{t_i=0}^{t}\theta_{G1}(t_i)\right\rangle \quad (4)$$

DOI: 10.1021/acs.jpcb.5b02579
J. Phys. Chem. B 2015, 119, 10597−10606

The anisotropy decays of the G1′ O−D groups are also plotted in Figure 2. The data show that the G1′ anisotropy decays are even slower than the G1 decays. Since the anisotropy decay difference between the G1 and G1′ O−D groups arises from the O−D groups whose O−D···O_{TMAO} hydrogen-bond is broken, the G1′ dynamics being slower than the G1 dynamics indicates that hydrogen-bond breaking contributes to the anisotropy decay of the O−D groups with the O−D···O_{TMAO} hydrogen-bond; in other words, the difference of the G1 and G1′ anisotropy decays provide evidence for the contribution of mechanism i.

The anisotropy decay of the G1′ O−D groups is slow, but the G1′ O−D groups still certainly lose the orientational information. To address the process of losing the orientational memory of the O−D groups while keeping the O−D···O_{TMAO} hydrogen-bond intact, we compared the anisotropy decays of the G1′ O−D groups and the O−N group of the TMAO molecule. To calculate the anisotropy decay of the TMAO molecule with the same ensemble used for the calculation of the G1′ O−D groups, we used the projection of the G1′ O−D vector onto the O−N group of the TMAO molecule. In this manner, we exclude any bias due to hydrogen-bond dissociation events of water molecules that are in G1 but not in G1′. Such dissociation events allow for N−O rotation while keeping the O−D(G1′)···O−N geometry unchanged. In contrast to the N−O vector, the projection of the G1′ O−D vector onto the N−O vector directly maps the binding geometry between the water molecules in G1′ and the TMAO molecules and thus directly represents the orientational degree of freedom within the hydrogen-bonded complex. The anisotropy decay for the projected G1′ O−D bond is given by

$$C_{TMAO}(t) = \frac{2}{5}\left\langle P_2\left(\frac{\mathbf{r}_{OD(p)}(t)\cdot\mathbf{r}_{OD(p)}(0)}{|\mathbf{r}_{OD(p)}(t)||\mathbf{r}_{OD(p)}(0)|}\right)\prod_{t_i=0}^{t}\theta_{G1}(t_i)\right\rangle \quad (5)$$

$$\mathbf{r}_{OD(p)}(t) = (\mathbf{r}_{ON}(t)\cdot\mathbf{r}_{OD}(t))\mathbf{r}_{ON}(t) \quad (6)$$

where $\boldsymbol{r}_{OD(p)}(t)$ denotes the projected G1′ O−D group at time t. Since $\boldsymbol{r}_{OD(p)}(t)$ is parallel to the O−N group of the TMAO molecule, the anisotropy decay given by eq 5 represents the TMAO rotation.

The TMAO anisotropy calculated using eq 5 is depicted in Figure 4, along with the G1 and G1′ anisotropy decays. The time constants for the decays are listed in Table 2. The very strong similarity between the anisotropy decays for the G1′ O−D group

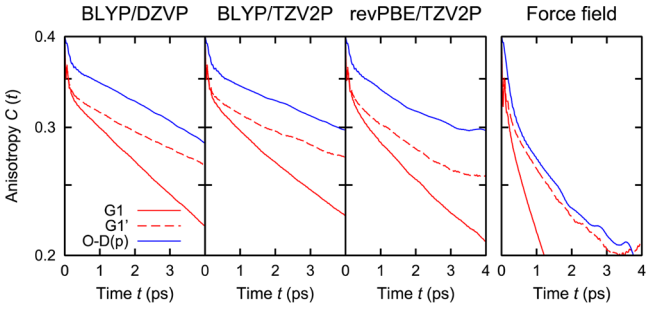

Figure 4. Semilog plots of simulated anisotropy decays of the TMAO molecules with long-lived hydrogen-bonds (with O−D groups in the G1′ subensemble). For comparison, the G1 and G1′ anisotropy decays are also plotted in red.

Table 2. Time Constants τ (ps) of the Anisotropy Decays[a]

	BLYP/DZVP	BLYP/TZV2P	revPBE/TZV2P	force field
G1	9.3	10	8.5	3.0
G1′	17	19	13	7.3
G2 (5 Å)	4.8	4.4	2.8	2.5
G2 (3 Å)	5.3	4.8	2.9	2.8
G3	3.9	3.6	2.3	2.0
O−D(p)	16	21	16	7.3
pure D_2O	3.9	3.3	2.1	2.2

[a]The decays were fit with the exponential decay $C(t) = A\exp(-t/\tau)$ for 0.5−3.0 ps.

and the TMAO (projected G1′ O−D groups) illustrate that the G1′ anisotropy decay is governed by the TMAO rotation: the O−D groups with keeping the hydrogen-bond to the O_{TMAO} atom intact rotate together with the TMAO molecule.

The very slow rotational motion for those G1′ O−D groups that kept the O−D···O_{TMAO} hydrogen-bonds intact during the relevant time window in the AIMD simulations is qualitatively consistent with experiments. In time-resolved IR experiments using a red-shifted (2450 cm^{-1}) pump and probe pulses,[42] the reorientational motion of the O−D groups hydrogen-bonded to the O_{TMAO} atom can be probed. While the contribution of these oscillators is weak at low concentrations of TMAO, at high concentrations of TMAO the experiment preferentially probes the anisotropy decay of the G1′ O−D groups with the O−D···O_{TMAO} hydrogen-bond. At high TMAO concentrations, the experimentally measured anisotropy decay by pumping the 2450 cm^{-1} IR band seems to support the pronounced slow-down of the G1 O−D groups.[42] Note however that since the VDOS at 2450 cm^{-1} includes not only the G1 O−D groups but also the O−D groups which do not interact with the O_{TMAO} atoms, the simulations can only be qualitatively compared to the experiment at low concentrations. Nevertheless, in particular, the much slower rotation of water molecules hydrogen-bonded to the O_{TMAO} atom is supported by a steplike decay of the anisotropy at intermediate concentrations of TMAO[42] and has also been inferred from nuclear Overhauser effect spectroscopy measument,[80] experimentally measured density and activity coefficient data,[23] and dielectric relaxation data.[42,47] This leads to the notion that the immobilized water molecule arises from the strong O−D···O_{TMAO} hydrogen-bond. However, to allow a direct comparison between the simulation and the experiment, we would need to simulate the time-resolved anisotropy decay, requiring nonequilibrium AIMD techniques.

III.C. Hydrogen-Bond Dynamics. As discussed above, the difference between the G1 and G1′ anisotropy decays represents the orientational information loss due to the breaking of the O−D···O_{TMAO} hydrogen-bonds (lower pathway in Figure 3). We have already pointed out that the contribution of this pathway to the G1 anisotropy decay is larger in the force field MD simulation than in the AIMD simulations, as is clear in Figure 2. To compare, in more detail, the hydrogen-bond dynamics in the force field MD and AIMD, we calculated the hydrogen-bond correlation function[84]

$$p_{HB}(t) = \frac{\langle h(0)h(t)\rangle}{\langle h(0)\rangle} \quad (7)$$

where the hydrogen-bond formation function, $h(t)$, was 1 when 1.59 Å < $r_{O\cdots D}$ < 2.27 Å,[77,78] and 0 otherwise. $r_{O\cdots D}$ denotes the intermolecular $O_{TMAO}\cdots D_{D2O}$ distance for the TMAO solution

DOI: 10.1021/acs.jpcb.5b02579
J. Phys. Chem. B 2015, 119, 10597−10606

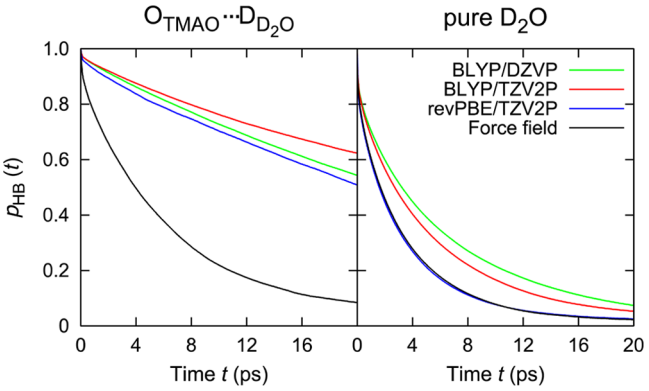

Figure 5. (Left) O−D···O_{TMAO} hydrogen-bond correlation functions in the aqueous TMAO solution. (Right) O···D hydrogen-bond correlation functions in pure D_2O.

and intermolecular O···D distance for the pure D_2O. The result of this analysis is plotted in Figure 5. For the aqueous TMAO solution, the AIMD results yield remarkably long-lived O−D···O_{TMAO} hydrogen-bonds, while the force field MD shows much faster hydrogen-bond breaking dynamics. Very interestingly, the differences are not so pronounced for pure D_2O. This indicates that the O−D···O_{TMAO} hydrogen-bond is qualitatively different from the water−water hydrogen-bonds, and while the force field simulation describes the water−water interaction quite well, the force field simulation seems less appropriate for describing the O−D···O_{TMAO} interaction. The hydrogen-bond lifetimes for the TMAO solution and pure D_2O are summarized in Table 3.

Table 3. Hydrogen-Bond Lifetimes τ of AIMD and Force Field MD Trajectories Calculated by Fitting the Exponential Function of $A\exp(-t/\tau)$ to the Data in the Range 0.5 ps < t < 20 ps[a]

	BLYP/ DZVP	BLYP/ TZV2P	revPBE/ TZV2P	force field
O−D···O_{TMAO}	35	45	33	7.6
pure D_2O	7.8	6.5	4.3	4.3

[a]The unit is in picoseconds.

The lifetimes for the O−D···O_{TMAO} hydrogen-bond of 30−50 ps predicted with the AIMD trajectories at 320 K are in broad concordance with dielectric spectroscopy experiments which indicated that at least two of the three hydrogen-bonds between water and TMAO remain intact for at least 50 ps at ∼300 K.[42,47] Note that the temperature difference of 20 K varies the D_2O dynamics in the TMAO hydration shell by at most 20% of the apparent activation energy for rotation.[46] The 20% variation is within the error bar for the simulated anisotropy decay with the different functionals/basis sets. Furthermore, since it is known that, in contrast to revPBE-AIMD, the BLYP-AIMD simulation predicts slightly overstructured water even with the van der Waals corrections, the comparison between the BLYP-AIMD simulation, force field MD simulation, and experiment has been previously made by setting the temperature of the BLYP-AIMD simulation by 15−30 K higher than the force field MD simulation and/or experiment, to thermally "loosen" the water structure.[85,86] At these elevated temperatures, the reorientation of water is sped up by ∼10%,[30,87,88] compared to 300 K, so that the true discrepancy between the BLYP-AIMD and force field MD is slightly overestimated here, but the qualitative difference remains, as does the conclusion drawn from our study, that the directionality of the hydrogen-bond between water and TMAO may need to be accounted for to describe the TMAO hydration dynamics adequately.

III.D. Angle-Resolved RDFs. From the details above, it is apparent that there are substantial differences between the O−D···O_{TMAO} hydrogen-bond dynamics in the AIMD and force field MD simulations. To explore possible structural differences predicted by the two models, we calculated the angle-resolved RDFs from the MD trajectories. The angle-resolved RDF of the D atoms of the D_2O molecules with respect to the O_{TMAO} atom can be calculated as

$$f(r,\theta) = \frac{1}{2\pi r^2 \cdot \Delta\cos\theta \cdot \Delta r}\frac{V}{N}\langle \Delta N(r,\cos\theta)\rangle \quad (8)$$

where, for the aqueous TMAO solution, r is the $O_{TMAO}\cdots D_{D2O}$ distance and $\theta(0° \le \theta \le 180°)$ is the angle between the O_{TMAO}−N vector of the dTMAO molecule and the intermolecular $O_{TMAO}\cdots D_{D2O}$ vector. We also calculated the angle-resolved RDFs for pure D_2O by using eq 8, where r is the intermolecular O···D distance and θ is the angle between the intramolecular O−D vector and intermolecular O···D vector with the same O atom. $\Delta N(r, \cos\theta)$ is the number of the D atoms of the D_2O molecules that are in the volume element centered on $(r, \cos\theta)$. The calculated RDFs are displayed in Figure 6.

This figure shows that in the AIMD simulations the D atom is geometrically localized (the distribution peaks rather sharply

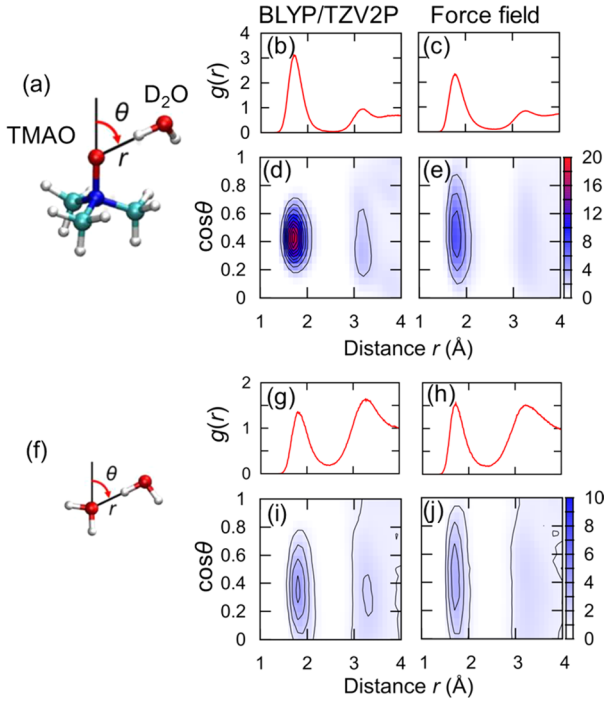

Figure 6. RDFs and angle-resolved RDFs for the D_{D2O} atoms (a−e) in the TMAO−D_2O solution and (f−i) in the pure D_2O calculated with the AIMD simulations at BLYP/TZV2P and the force field MD simulations. (a, f) Schematic pictures for the distance and angle, (b, c, g, h) RDFs, and (d, e, i, j) angle-resolved RDFs. The peak heights of the first hydration shells in the angle-resolved RDF are 19.5 for the AIMD (d) and 7.8 for the force field MD (e) for the TMAO solution, whereas for the pure D_2O the peak heights are 4.4 for the AIMD (i) and 3.7 for the force field MD (j).

DOI: 10.1021/acs.jpcb.5b02579
J. Phys. Chem. B 2015, 119, 10597−10606

at $\theta \approx 63°$), while in the force field MD simulation the location of the D atoms is broadly distributed. This clearly demonstrates that, in the AIMD simulations, the O−D···O_{TMAO} hydrogen-bonds display a specific directionality, in contrast to the force field MD simulation. As is evident from the angle $\theta \approx 63°$, this directionality arises from the sp^3 orbital of the O_{TMAO} atom. The directionality of the O−D···O_{TMAO} hydrogen-bonds is not reproduced well with the force field model because of the spherically uniform electrostatic field generated by the atomic charge on the O_{TMAO} atom. The difference between the AIMD and force field MD is much less pronounced for the RDF of the bulk D_2O, explaining why both models largely agree in their description of pure D_2O. The difference between the oxygen atoms in TMAO and in pure water is that the former has three lone electron pairs and carries a formal negative charge, whereas the latter has two lone pairs, with no formal charge. These results indicate that care must be taken when describing the interaction with a negatively charged oxygen atom bound within the molecule by a single covalent bond. Note that the weaker hydrogen-bond O−D···O_{TMAO} in the force field MD simulation with the Kast model has been pointed out from the osmotic activity data.[15,37] Although several force field models have been recently presented and may provide qualitatively different results,[37,89] the atom charges have been located at the O_{TMAO} atom site in these models, inevitably generating a spherical electric field around the O_{TMAO} atom. This is likely the main difference between the AIMD from force field simulations. To reproduce the sp^3 directionality of the O−D···O_{TMAO} hydrogen-bond, a charge may be located at a virtual site, which has been frequently done in the four and five site water model such as TIP4P[90,91] and TIP5P.[92] The results obtained from our AIMD simulation offer a useful reference for constructing a force field model with virtual site charges to reproduce the directionality of the hydrogen-bonds. Our AIMD results thus provide a measure for validating these force fields and a guideline for further improving them.

III.E. Functional/Basis Set Dependence of Anisotropy Decays in Aqueous TMAO Solutions. The influence of the DFT functional/basis set on the static and dynamical properties of pure liquid water have been reported,[93−96] but the survey on the aqueous solutions has not been made. Here we briefly comment on the effect of the choice of the DFT functionals/basis set on the water dynamics in the TMAO solutions. Figure 2 shows that the revPBE yields slightly faster dynamics than BLYP in all the cases, including G1, G2, G3, and pure D_2O. The shorter time constants of the anisotropy decay of the pure D_2O with the revPBE are consistent with previous observations.[70] From this observation, we can conclude that this trend of the water dynamics for the different DFT functionals is observed for pure water as well as for aqueous TMAO solution. Furthermore, our simulation (Figure 2) indicates that the different basis sets (DZVP and TZV2P) do not give qualitatively different dynamics for both aqueous solution of TMAO and pure water.

IV. CONCLUSIONS

We have performed AIMD simulations of D_2O solutions of dTMAO in order to shed light on the water dynamics near the TMAO molecule. The 160 cm^{-1} red-shift of the O−D stretch vibration due to the O−D···O_{TMAO} hydrogen-bond predicted with the AIMD trajectories is in reasonable agreement with experiments,[19,50] whereas the force field failed to reproduce this large red-shift, indicating that *ab initio* modeling of the hydrogen-bonds between TMAO and D_2O is required to describe the water−hydrophilic TMAO part accurately. Our AIMD simulation predicts a very slow rotational motion for the G1 O−D groups hydrogen-bonded to the O_{TMAO} atom. We reveal that those G1 O−D groups can rotate in the following two ways: by keeping the O−D···O_{TMAO} hydrogen-bond, the O−D group will rotate along with the entire TMAO molecule. Alternatively, by breaking this hydrogen-bond, the O−D group can dissociate from the O_{TMAO} atom and rotate.

We have also discussed why this dynamics may not have been properly described by force field models. The force field model predicts much faster rotational dynamics for the G1 O−D groups and shorter lifetimes of the O−D···O_{TMAO} hydrogen-bond than the AIMD. Note that the rotational dynamics and hydrogen-bond breaking dynamics simulated with the AIMD and force field MD simulations are quite similar in pure D_2O. This qualitative difference of the water dynamics arises from the orbital directionality of the hydrogen-bond near the O_{TMAO} atom. In the AIMD simulation, the directional hydrogen-bonding originates from the sp^3 configuration of O_{TMAO}, which is not reproduced by the point charges employed in the force field MD simulation. Due to the spherically distributed electrostatic field in the force field model the O−D···O_{TMAO} hydrogen-bond is less directional.

Our simulations demonstrate that the strongly retarded reorientational dynamics of water molecules in the TMAO solution arise from the strong O−D···O_{TMAO} hydrogen-bond. This strong interaction of TMAO with water seems to be essential for understanding the indirect mechanism by which TMAO stabilizes protein structure.

AUTHOR INFORMATION

Corresponding Author

*E-mail: nagata@mpip-mainz.mpg.de.

Notes

The authors declare no competing financial interest.

ACKNOWLEDGMENTS

We are grateful for fruitful discussions with Dr. Aoife Fogarty, Dr. Raffaello Potestio, and Dr. Hisao Nakamura. K.U. also acknowledges the financial support from the Max Planck Graduate Center with Johannes Gutenberg University of Mainz. M.S. and Y.N. thank the German Science Foundation through the project of TRR 146.

REFERENCES

(1) Zou, Q.; Bennion, B. J.; Daggett, V.; Murphy, K. P. The Molecular Mechanism of Stabilization of Proteins by TMAO and Its Ability to Counteract the Effects of Urea. *J. Am. Chem. Soc.* **2002**, *124*, 1192−1202.

(2) Canchi, D. R.; García, A. E. Cosolvent Effects on Protein Stability. *Annu. Rev. Phys. Chem.* **2013**, *64*, 273−293.

(3) Levine, Z. A.; Larini, L.; LaPointe, N. E.; Feinstein, S. C.; Shea, J.-E. Regulation and Aggregation of Intrinsically Disordered Peptides. *Proc. Natl. Acad. Sci. U. S. A.* **2015**, *112*, 2758−2763.

(4) Denning, E. J.; Thirumalai, D.; Mackerell, A. D., Jr. Protonation of Trimethylamine N-Oxide (TMAO) Is Required for Stabilization of RNA Tertiary Structure. *Biophys. Chem.* **2013**, *184*, 8−16.

(5) Yancey, P. H. Organic Osmolytes as Compatible, Metabolic and Counteracting Cytoprotectants in High Osmolarity and Other Stresses. *J. Exp. Biol.* **2005**, *208*, 2819−2830.

(6) Ganguly, P.; Hajari, T.; Shea, J.-E.; van der Vegt, N. F. A. Mutual Exclusion of Urea and Trimethylamine *N*-Oxide from Amino Acids in Mixed Solvent Environment. *J. Phys. Chem. Lett.* **2015**, *6*, 581−585.

DOI: 10.1021/acs.jpcb.5b02579
J. Phys. Chem. B 2015, 119, 10597−10606

(7) Yancey, P. H. Water Stress, Osmolytes and Proteins. *Integr. Comp. Biol.* **2001**, *41*, 699−709.
(8) Yancey, P. H.; Blake, W. R.; Conley, J. Unusual Organic Osmolytes in Deep-Sea Animals: Adaptations to Hydrostatic Pressure and Other Perturbants. *Comp. Biochem. Physiol., Part A: Mol. Integr. Physiol.* **2002**, *133*, 667−676.
(9) Gillett, M. B.; Suko, J. R.; Santoso, F. O.; Yancey, P. H. Elevated Levels of Trimethylamine Oxide in Muscles of Deep-Sea Gadiform Teleosts: A High-Pressure Adaptation? *J. Exp. Zool.* **1997**, *279*, 386−391.
(10) Bennion, B. J.; Daggett, V. Counteraction of Urea-Induced Protein Denaturation by Trimethylamine N-Oxide: A Chemical Chaperone at Atomic Resolution. *Proc. Natl. Acad. Sci. U. S. A.* **2004**, *101*, 6433−6438.
(11) Auton, M.; Bolen, D. W. Predicting the Energetics of Osmolyte-Induced Protein Folding/unfolding. *Proc. Natl. Acad. Sci. U. S. A.* **2005**, *102*, 15065−15068.
(12) Auton, M.; Bolen, D. W.; Rösgen, J. Structural Thermodynamics of Protein Preferential Solvation: Osmolyte Solvation of Proteins, Aminoacids, and Peptides. *Proteins: Struct., Funct., Genet.* **2008**, *73*, 802−813.
(13) Courtenay, E. S.; Capp, M. W.; Anderson, C. F.; Record, M. T., Jr. Vapor Pressure Osmometry Studies of Osmolyte-Protein Interactions: Implications for the Action of Osmoprotectants in Vivo and for the Interpretation of "Osmotic Stress" Experiments in Vitro. *Biochemistry* **2000**, *39*, 4455−4471.
(14) Bolen, D. W.; Baskakov, I. V. The Osmophobic Effect: Natural Selection of a Thermodynamic Force in Protein Folding. *J. Mol. Biol.* **2001**, *310*, 955−963.
(15) Canchi, D. R.; Jayasimha, P.; Rau, D. C.; Makhatadze, G. I.; Garcia, A. E. Molecular Mechanism for the Preferential Exclusion of TMAO from Protein Surfaces. *J. Phys. Chem. B* **2012**, *116*, 12095−12104.
(16) Hunger, J.; Ottosson, N.; Mazur, K.; Bonn, M.; Bakker, H. J. Water-Mediated Interactions between Trimethylamine-*N*-Oxide and Urea. *Phys. Chem. Chem. Phys.* **2015**, *17*, 298−306.
(17) Comez, L.; Lupi, L.; Morresi, A.; Paolantoni, M.; Sassi, P.; Fioretto, D. More Is Different: Experimental Results on the Effect of Biomolecules on the Dynamics of Hydration Water. *J. Phys. Chem. Lett.* **2013**, *4*, 1188−1192.
(18) Mondal, J.; Stirnemann, G.; Berne, B. J. When Does Trimethylamine *N*-Oxide Fold a Polymer Chain and Urea Unfold It? *J. Phys. Chem. B* **2013**, *117*, 8723−8732.
(19) Panuszko, A.; Bruździak, P.; Zielkiewicz, J.; Wyrzykowski, D.; Stangret, J. Effects of Urea and Trimethylamine-*N*-Oxide on the Properties of Water and the Secondary Structure of Hen Egg White Lysozyme. *J. Phys. Chem. B* **2009**, *113*, 14797−14809.
(20) Gluick, T. C.; Yadav, S. Trimethylamine *N*-Oxide Stabilizes RNA Tertiary Structure and Attenuates the Denaturating Effects of Urea. *J. Am. Chem. Soc.* **2003**, *125*, 4418−4419.
(21) Kokubo, H.; Hu, C. Y.; Pettitt, B. M. Peptide Conformational Preferences in Osmolyte Solutions: Transfer Free Energies of Decaalanine. *J. Am. Chem. Soc.* **2011**, *133*, 1849−1858.
(22) O'Brien, E. P.; Ziv, G.; Haran, G.; Brooks, B. R.; Thirumalai, D. Effects of Denaturants and Osmolytes on Proteins Are Accurately Predicted by the Molecular Transfer Model. *Proc. Natl. Acad. Sci. U. S. A.* **2008**, *105*, 13403−13408.
(23) Rösgen, J.; Jackson-Atogi, R. Volume Exclusion and H-Bonding Dominate the Thermodynamics and Solvation of Trimethylamine-*N*-Oxide in Aqueous Urea. *J. Am. Chem. Soc.* **2012**, *134*, 3590−3597.
(24) Mondal, J. A.; Nihonyanagi, S.; Yamaguchi, S.; Tahara, T. Three Distinct Water Structures at a Zwitterionic Lipid/water Interface Revealed by Heterodyne-Detected Vibrational Sum Frequency Generation. *J. Am. Chem. Soc.* **2012**, *134*, 7842−7850.
(25) Stirnemann, G.; Sterpone, F.; Laage, D. Dynamics of Water in Concentrated Solutions of Amphiphiles: Key Roles of Local Structure and Aggregation. *J. Phys. Chem. B* **2011**, *115*, 3254−3262.
(26) Kuffel, A.; Zielkiewicz, J. The Hydrogen Bond Network Structure within the Hydration Shell around Simple Osmolytes: Urea, Tetramethylurea, and Trimethylamine-*N*-Oxide, Investigated Using Both a Fixed Charge and a Polarizable Water Model. *J. Chem. Phys.* **2010**, *133*, 035102.
(27) Doi, H.; Watanabe, Y.; Aida, M. Influence of Trimethylamine N-Oxide (TMAO) on the Three-Dimensional Distribution and Alignment of Solvent Molecules in Aqueous Solution. *Chem. Lett.* **2014**, *43*, 865−867.
(28) Stirnemann, G.; Hynes, J. T.; Laage, D. Water Hydrogen Bond Dynamics in Aqueous Solutions of Amphiphiles. *J. Phys. Chem. B* **2010**, *114*, 3052−3059.
(29) Laage, D.; Stirnemann, G.; Hynes, J. T. Why Water Reorientation Slows without Iceberg Formation around Hydrophobic Solutes. *J. Phys. Chem. B* **2009**, *113*, 2428−2435.
(30) Duboué-Dijon, E.; Fogarty, A. C.; Laage, D. Temperature Dependence of Hydrophobic Hydration Dynamics: From Retardation to Acceleration. *J. Phys. Chem. B* **2014**, *118*, 1574−1583.
(31) Paul, S.; Patey, G. N. The Influence of Urea and Trimethylamine-*N*-Oxide on Hydrophobic Interactions. *J. Phys. Chem. B* **2007**, *111*, 7932−7933.
(32) Paul, S.; Patey, G. N. Structure and Interaction in Aqueous Urea-Trimethylamine-*N*-Oxide Solutions. *J. Am. Chem. Soc.* **2007**, *129*, 4476−4482.
(33) Paul, S.; Patey, G. N. Why Tert-Butyl Alcohol Associates in Aqueous Solution but Trimethylamine-*N*-Oxide Does Not. *J. Phys. Chem. B* **2006**, *110*, 10514−10518.
(34) Biyani, N.; Paul, S. Hydrophobic Interactions in Water-Trimethylamine-*N*-Oxide Solutions: The Effects of Pressure. *J. Phys. Chem. B* **2009**, *113*, 9644−9645.
(35) Sharp, K. A.; Madan, B.; Manas, E.; Vanderkooi, J. M. Water Structure Changes Induced by Hydrophobic and Polar Solutes Revealed by Simulations and Infrared Spectroscopy. *J. Chem. Phys.* **2001**, *114*, 1791−1796.
(36) Sinibaldi, R.; Casieri, C.; Melchionna, S.; Onori, G.; Segre, A. L.; Viel, S.; Mannina, L.; De Luca, F. The Role of Water Coordination in Binary Mixtures. a Study of Two Model Amphiphilic Molecules in Aqueous Solutions by Molecular Dynamics and NMR. *J. Phys. Chem. B* **2006**, *110*, 8885−8892.
(37) Schneck, E.; Horinek, D.; Netz, R. R. Insight into the Molecular Mechanisms of Protein Stabilizing Osmolytes from Global Force-Field Variations. *J. Phys. Chem. B* **2013**, *117*, 8310−8321.
(38) Freda, M.; Onori, H.; Santucci, A. Infrared and Dielectric Spectroscopy Study of the Water Perturbation Induced by Two Small Organic Solutes. *J. Mol. Struct.* **2001**, *565*−*566*, 153−157.
(39) Freda, M.; Onori, G.; Santucci, A. Infrared Study of the Hydrophobic Hydration and Hydrophobic Interactions in Aqueous Solutions of *tert*-Butyl Alcohol and Trimethylamine-*n*-Oxide. *J. Phys. Chem. B* **2001**, *105*, 12714−12718.
(40) Rezus, Y. L. A.; Bakker, H. J. Observation of Immobilized Water Molecules around Hydrophobic Groups. *Phys. Rev. Lett.* **2007**, *99*, 148301.
(41) Rezus, Y. L. A.; Bakker, H. J. Destabilization of the Hydrogen-Bond Structure of Water by the Osmolyte Trimethylamine *N*-Oxide. *J. Phys. Chem. B* **2009**, *113*, 4038−4044.
(42) Hunger, J.; Tielrooij, K. J.; Buchner, R.; Bonn, M.; Bakker, H. J. Complex Formation in Aqueous Trimethylamine-*N*-Oxide (TMAO) Solutions. *J. Phys. Chem. B* **2012**, *116*, 4783−4795.
(43) Bakulin, A. A.; Pshenichnikov, M. S.; Bakker, H. J.; Petersen, C. Hydrophobic Molecules Slow down the Hydrogen-Bond Dynamics of Water. *J. Phys. Chem. A* **2011**, *115*, 1821−1829.
(44) Munroe, K. L.; Magers, D. H.; Hammer, N. I. Raman Spectroscopic Signatures of Noncovalent Interactions between Trimethylamine N-Oxide (TMAO) and Water. *J. Phys. Chem. B* **2011**, *115*, 7699−7707.
(45) Mazur, K.; Heisler, I. A.; Meech, S. R. THz Spectra and Dynamics of Aqueous Solutions Studied by the Ultrafast Optical Kerr Effect. *J. Phys. Chem. B* **2011**, *115*, 2563−2573.
(46) Qvist, J.; Halle, B. Thermal Signature of Hydrophobic Hydration Dynamics. *J. Am. Chem. Soc.* **2008**, *130*, 10345−10353.

DOI: 10.1021/acs.jpcb.5b02579
J. Phys. Chem. B 2015, 119, 10597−10606

(47) Shikata, T.; Itatani, S. Dielectric Relaxation of Aqueous Trimethylamineoxide Solutions. *J. Solution Chem.* **2002**, *31*, 823−844.
(48) Silvestrelli, P. L. Are There Immobilized Water Molecules around Hydrophobic Groups? Aqueous Solvation of Methanol from First Principles. *J. Phys. Chem. B* **2009**, *113*, 10728−10731.
(49) Sterpone, F.; Stirnemann, G.; Hynes, J. T.; Laage, D. Water Hydrogen-Bond Dynamics around Amino Acids: The Key Role of Hydrophilic Hydrogen-Bond Acceptor Groups. *J. Phys. Chem. B* **2010**, *114*, 2083−2089.
(50) Figure 5 of ref 19 exhibits the IR spectrum of aqueous TMAO solution, where the IR spectrum was fit with several Gaussians. One Gaussian has the peak frequency similar to the peak frequency of bulk water, while the other OD stretch peaks show a strong (exceeding 100 cm^{-1}) red-shift. Since these red-shifted peaks can be assigned to the water−TMAO interaction, one can expect that TMAO−water interactions give rise to the red-shifted peak over 100 cm^{-1}. Figure 4 of ref 39 shows a red-shift of > 400 cm^{-1} for the O−H stretch mode corresponding to a red-shift of ∼290 cm^{-1} in the O−D stretch mode. The transient IR spectrum (Figure 10) in ref 42 shows the red-shift of ∼55 cm^{-1} by the transient spectra.
(51) Laage, D.; Hynes, J. T. A Molecular Jump Mechanism of Water Reorientation. *Science* **2006**, *311*, 832−835.
(52) Fogarty, A. C.; Duboué-Dijon, E.; Sterpone, F.; Hynes, J. T.; Laage, D. Biomolecular Hydration Dynamics: A Jump Model Perspective. *Chem. Soc. Rev.* **2013**, *42*, 5672−5683.
(53) Laage, D.; Hynes, J. T. Reorientional Dynamics of Water Molecules in Anionic Hydration Shells. *Proc. Natl. Acad. Sci. U. S. A.* **2007**, *104*, 11167−11172.
(54) Fogarty, A. C.; Coudert, F. X.; Boutin, A.; Laage, D. Reorientational Dynamics of Water Confined in Zeolites. *ChemPhysChem* **2014**, *15*, 521−529.
(55) Laage, D.; Hynes, J. T. Do More Strongly Hydrogen-Bonded Water Molecules Reorient More Slowly? *Chem. Phys. Lett.* **2006**, *433*, 80−85.
(56) Laage, D.; Hynes, J. T. On the Molecular Mechanism of Water Reorientation. *J. Phys. Chem. B* **2008**, *112*, 14230−14242.
(57) Fogarty, A. C.; Duboué-Dijon, E.; Laage, D.; Thompson, W. H. Origins of the Non-Exponential Reorientation Dynamics of Nanoconfined Water. *J. Chem. Phys.* **2014**, *141*, 18C523.
(58) Berendsen, H. J. C.; Grigera, J. R.; Straatsma, T. P. The Missing Term in Effective Pair Potentials. *J. Phys. Chem.* **1987**, *91*, 6269−6271.
(59) Kast, K. M.; Brickmann, J.; Kast, S. M.; Berry, R. S. Binary Phases of Aliphatic *N*-Oxides and Water: Force Field Development and Molecular Dynamics Simulation. *J. Phys. Chem. A* **2003**, *107*, 5342−5351.
(60) Kocherbitov, V.; Veryazov, V.; Söderman, O. Hydration of Trimethylamine-*N*-Oxide and of Dimethyldodecylamine-*N*-Oxide: An *ab Initio* Study. *J. Mol. Struct.: THEOCHEM* **2007**, *808*, 111−118.
(61) Lee, H.-S.; Tuckerman, M. E. Dynamical Properties of Liquid Water from *ab Initio* Molecular Dynamics Performed in the Complete Basis Set Limit. *J. Chem. Phys.* **2007**, *126*, 164501.
(62) Chandra, A.; Tuckerman, M. E.; Marx, D. Connecting Solvation Shell Structure to Proton Transport Kinetics in Hydrogen-Bonded Networks via Population Correlation Functions. *Phys. Rev. Lett.* **2007**, *99*, 145901.
(63) Makarov, D. M.; Egorov, G. I.; Kolker, A. M. Density and Volumetric Properties of Aqueous Solutions of Trimethylamine *N*-Oxide in the Temperature Range from (278.15 to 323.15) K and at Pressures up to 100 MPa. *J. Chem. Eng. Data* **2015**, *60*, 1291−1299.
(64) Bussi, G.; Donadio, D.; Parrinello, M. Canonical Sampling through Velocity Rescaling. *J. Chem. Phys.* **2007**, *126*, 014101.
(65) CP2K developers group. *CP2K*; http://www.cp2k.org/ (accessed May 10, 2015).
(66) Becke, A. D. Density-Functional Exchange-Energy Approximation with Correct Asymptotic Behavior. *Phys. Rev. A: At., Mol., Opt. Phys.* **1988**, *38*, 3098−3100.
(67) Lee, C.; Yang, W.; Parr, R. G. Development of the Colle-Salvetti Correlation-Energy Formula into a Functional of the Electron Density. *Phys. Rev. B: Condens. Matter Mater. Phys.* **1988**, *37*, 785−789.
(68) Zhang, Y.; Yang, W. Comment on "Generalized Gradient Approximation Made Simple. *Phys. Rev. Lett.* **1998**, *80*, 890−890.
(69) Grimme, S.; Antony, J.; Ehrlich, S.; Krieg, H. A Consistent and Accurate Ab Initio Parametrization of Density Functional Dispersion Correction (DFT-D) for the 94 Elements H-Pu. *J. Chem. Phys.* **2010**, *132*, 154104.
(70) Lin, I.-C.; Seitsonen, A. P.; Tavernelli, I.; Rothlisberger, U. Structure and Dynamics of Liquid Water from Ab Initio Molecular Dynamics-Comparison of BLYP, PBE, and revPBE Density Functionals with and without van Der Waals Corrections. *J. Chem. Theory Comput.* **2012**, *8*, 3902−3910.
(71) Lin, I.-C.; Seitsonen, A. P.; Coutinho-Neto, M. D.; Tavernelli, I.; Rothlisberger, U. Importance of van Der Waals Interactions in Liquid Water. *J. Phys. Chem. B* **2009**, *113*, 1127−1131.
(72) Kühne, T. D.; Pascal, T. A.; Kaxiras, E.; Jung, Y. New Insights into the Structure of the Vapor/water Interface from Large-Scale First-Principles Simulations. *J. Phys. Chem. Lett.* **2011**, *2*, 105−113.
(73) Goedecker, S.; Teter, M.; Hutter, J. Separable Dual-Space Gaussian Pseudopotentials. *Phys. Rev. B: Condens. Matter Mater. Phys.* **1996**, *54*, 1703−1710.
(74) Vandevondele, J.; Krack, M.; Mohamed, F.; Parrinello, M.; Chassaing, T.; Hutter, J. Quickstep: Fast and Accurate Density Functional Calculations Using a Mixed Gaussian and Plane Waves Approach. *Comput. Phys. Commun.* **2005**, *167*, 103−128.
(75) Jonchiere, R.; Seitsonen, A. P.; Ferlat, G.; Saitta, A. M.; Vuilleumier, R. Van Der Waals Effects in *ab Initio* Water at Ambient and Supercritical Conditions. *J. Chem. Phys.* **2011**, *135*, 154503.
(76) Wu, Y.; Tepper, H. L.; Voth, G. A. Flexible Simple Point-Charge Water Model with Improved Liquid-State Properties. *J. Chem. Phys.* **2006**, *124*, 024503.
(77) Kuo, I.-F. W.; Mundy, C. J. An Ab Initio Molecular Dynamics Study of the Aqueous Liquid-Vapor Interface. *Science* **2004**, *303*, 658−660.
(78) Kumar, R.; Schmidt, J. R.; Skinner, J. L. Hydrogen Bonding Definitions and Dynamics in Liquid Water. *J. Chem. Phys.* **2007**, *126*, 204107.
(79) Titantah, J. T.; Karttunen, M. Long-Time Correlations and Hydrophobe-Modified Hydrogen-Bonding Dynamics in Hydrophobic Hydration. *J. Am. Chem. Soc.* **2012**, *134*, 9362−9368.
(80) Hovagimyan, K. G.; Gerig, J. T. Interactions of Trimethylamine *N*-Oxide and Water with Cyclo-Alanylglycine. *J. Phys. Chem. B* **2005**, *109*, 24142−24151.
(81) Corcelli, S. A.; Lawrence, C. P.; Skinner, J. L. Combined Electronic Structure/molecular Dynamics Approach for Ultrafast Infrared Spectroscopy of Dilute HOD in Liquid H_2O and D_2O. *J. Chem. Phys.* **2004**, *120*, 8107−8117.
(82) Bakker, H. J.; Skinner, J. L. Vibrational Spectroscopy as a Probe of Structure and Dynamics in Liquid Water. *Chem. Rev.* **2010**, *110*, 1498−1517.
(83) Titantah, J. T.; Karttunen, M. Water Dynamics: Relation between Hydrogen Bond Bifurcations, Molecular Jumps, Local Density & Hydrophobicity. *Sci. Rep.* **2013**, *3*, 2991.
(84) Luzar, A.; Chandler, D. Hydrogen-Bond Kinetics in Liquid Water. *Nature* **1996**, *379*, 55−57.
(85) Sulpizi, M.; Salanne, M.; Sprik, M.; Gaigeot, M.-P. Vibrational Sum Frequency Generation Spectroscopy of the Water Liquid−Vapor Interface from Density Functional Theory-Based Molecular Dynamics Simulations. *J. Phys. Chem. Lett.* **2013**, *4*, 83−87.
(86) Nagata, Y.; Yoshimune, S.; Hsieh, C.-S.; Hunger, J.; Bonn, M. Ultrafast Vibrational Dynamics of Water Disentangled by Reverse Nonequilibrium Ab Initio Molecular Dynamics Simulations. *Phys. Rev. X* **2015**, *5*, 021002.
(87) Petersen, C.; Tielrooij, K.-J.; Bakker, H. J. Strong Temperature Dependence of Water Reorientation in Hydrophobic Hydration Shells. *J. Chem. Phys.* **2009**, *130*, 214511.
(88) Moilanen, D. E.; Fenn, E. E.; Lin, Y.-S.; Skinner, J. L.; Bagchi, B.; Fayer, M. D. Water Inertial Reorientation: Hydrogen Bond Strength and the Angular Potential. *Proc. Natl. Acad. Sci. U. S. A.* **2008**, *105*, 5295−5300.

DOI: 10.1021/acs.jpcb.5b02579
J. Phys. Chem. B 2015, 119, 10597−10606

(89) Larini, L.; Shea, J.-E. Double Resolution Model for Studying TMAO/water Effective Interactions. *J. Phys. Chem. B* **2013**, *117*, 13268−13277.
(90) Jorgensen, W. L.; Chandrasekhar, J.; Madura, J. D.; Impey, R. W.; Klein, M. L. Comparison of Simple Potential Functions for Simulating Liquid Water. *J. Chem. Phys.* **1983**, *79*, 926−935.
(91) Abascal, J. L.; Vega, C. A General Purpose Model for the Condensed Phases of Water: TIP4P/2005. *J. Chem. Phys.* **2005**, *123*, 234505.
(92) Mahoney, M. W.; Jorgensen, W. L. Quantum, Intramolecular Flexibility, and Polarizability Effects on the Reproduction of the Density Anomaly of Liquid Water by Simple Potential Functions. *J. Chem. Phys.* **2000**, *112*, 8910−8922.
(93) Schmidt, J.; Vandevondele, J.; Kuo, I. F. W.; Sebastiani, D.; Siepmann, J. I.; Hutter, J.; Mundy, C. J. Isobaric-Isothermal Molecular Dynamics Simulations Utilizing Density Functional Theory: An Assessment of the Structure and Density of Water at near-Ambient Conditions. *J. Phys. Chem. B* **2009**, *113*, 11959−11964.
(94) Kühne, T. D.; Krack, M.; Parrinello, M. Static and Dynamical Properties of Liquid Water from First Principles by a Novel Car-Parrinello-like Approach. *J. Chem. Theory Comput.* **2009**, *5*, 235−241.
(95) Del Ben, M.; Schönherr, M.; Hutter, J.; Vandevondele, J. Bulk Liquid Water at Ambient Temperature and Pressure from MP2 Theory. *J. Phys. Chem. Lett.* **2013**, *4*, 3753−3759.
(96) VandeVondele, J.; Mohamed, F.; Krack, M.; Hutter, J.; Sprik, M.; Parrinello, M. The Influence of Temperature and Density Functional Models in *ab Initio* Molecular Dynamics Simulation of Liquid Water. *J. Chem. Phys.* **2005**, *122*, 014515.

DOI: 10.1021/acs.jpcb.5b02579
J. Phys. Chem. B 2015, 119, 10597−10606